Classification of non-Gaussian diffusion profiles for HARDI data simplification

V. Prckovska[1], A. Vilanova[1], C. Poupon[2], B. ter Haar Romeny[1], and M. Descoteaux[3]
[1]Biomedical Engineering, Eindhoven University of Technology, Eindhoven, Netherlands, [2]NeuroSpin, CEA Saclay, Gif-sur-Yvette, France, [3]Computer Science, Université de Sherbrooke, Québec, Canada

INTRODUCTION: High angular resolution diffusion imaging (HARDI) is able to capture the water diffusion pattern in areas of complex intravoxel fiber configurations. However, compared to diffusion tensor imaging (DTI), HARDI adds extra complexity (e.g., high post-processing time and memory costs, nonintuitive visualization). Separating the data into Gaussian and non-Gaussian areas can allow using complex HARDI models just when it is necessary. We study HARDI anisotropy measures as classification criteria applied to different HARDI models. The chosen measures are fast to calculate and provide interactive data classification.

METHODS: We implemented several anisotropy measures from the literature, generalized anisotropy (GA)[1], generalized fractional anisotropy (GFA)[2], and the cumulative residual entropy (CRE)[3]. These measures were applied on the ADC profiles, analytical q-ball[4] and the DOT[1] all referred as spherical probability functions (SPFs). DOT has been adapted to be represented by real Spherical Harmonics, such that all the anisotropy measures can be applied equally. To avoid the R_0 selection problem in DOT and inspired by definitions of the Orientation Distribution Function (ODF) from Q-ball imaging [2] and the marginal ODF (mODF) from diffusion spectrum imaging (DSI)[5], we propose the similar ODFs computed from the DOT as: $\psi_{\text{DOT-ODF}(\vartheta,\varphi)}=\int_0^{R0max} P(r,\vartheta,\varphi)\mathrm{d}r$, $\psi_{\text{DOT-mODF}(\vartheta,\varphi)}=\int_0^{R0max} P(r,\vartheta,\varphi)r^2\mathrm{d}r$, where $P(r,\vartheta,\varphi)$ is the probability density function (PDF) computed from DOT and R_{0max} is set to a conservatively high value (see table on Figure 1 right). Furthermore, as a discrete binary measure for classification we propose to use the number of maxima (NM).

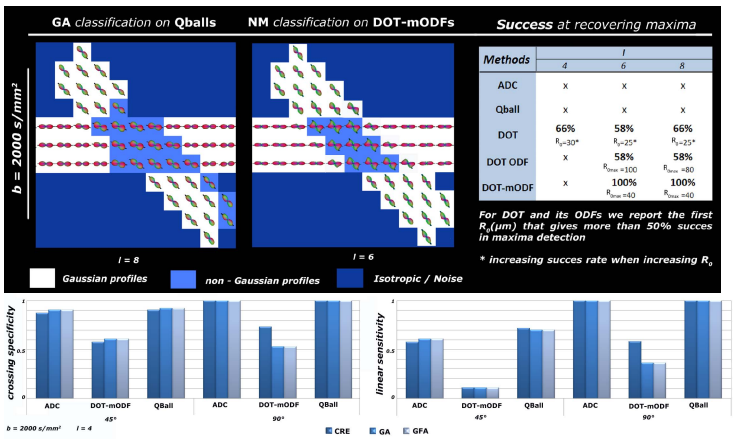

Figure 1. Classification results from the phantom data

DATA: ***Ex-vivo phantom***: We use two real physical *ex-vivo* phantoms with fibre bundles crossing at 45° and 90°[6]. We analyze the data acquired at two b-values of b=2000 and b=8000s/mm^2, along 200 uniform directions. ***Human***: Diffusion acquisitions were performed using a twice focused spin-echo echo-planar imaging sequence on a Siemens Allegra 3T scanner, with FOV 208X208 mm, isotropic voxels of 2mm. Uniform gradient direction schemes with 49 and 121 directions were used and the diffusion-weighted volumes were interleaved with b_0, volumes every 12th scanned gradient direction. Datasets were acquired at b-values of 1000, 1500, 2000, 3000, 4000 s/mm^2 and in the same session, two anatomical data sets (192 slices, isotropic 1mm voxels) were acquired using the ADNI protocol for registration. Finally, before ADC, q-balls and DOT reconstructions, we applied a denoising step available online (http://www.irisa.fr/visages/benchmarks/), to correct for the Rician noise bias in the datasets.

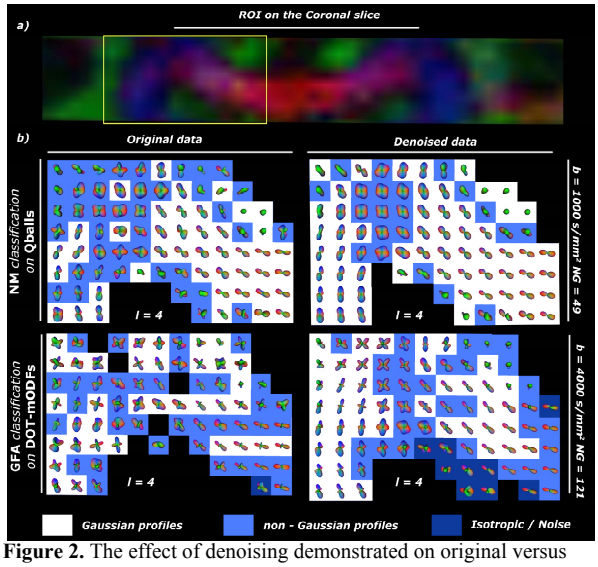

Figure 2. The effect of denoising demonstrated on original versus denoised data in different acquisition schemes

RESULTS: ***Phantom:*** DOT has the potential of recovering small angles regardless of the b-value, which we demonstrate in the table of Fig. 1. In the table we report the success at recovering two maxima in the crossing voxels by all of the examined SPFs. We observe that the derivations of the DOT (DOT-ODF and DOT-mODF) manifest similar behavior as the DOT itself, which shows a better angular resolution than q-ball and suggests a better choice of reconstruction algorithm for fiber tracking purpose. For the rest of the anisotropy measures, we can quantitatively describe the classification power of the 45° and 90° phantoms by using a binary classification statistical test. We report the specificity and sensitivity of the classified crossing and linear voxels respectively. Two thresholds are needed to separate the interval of anisotropy values into three distinct compartments: Isotropic/noise, Gaussian and non-Gaussian. We thus iterate over the whole range of values of each anisotropy measure and find the interval where all the crossings are detected while the number of false positives stays minimal. For the purpose of data simplification, the presence of false negatives is dangerous (i.e. crossings detected as linear), because relevant information can be lost. Therefore to ensure absence of false negatives, we set the sensitivity of crossing classification criteria to 1. In Fig. 1, bottom, we present the specificity of the crossing classification for each measure and the sensitivity of the linear detected voxels for the 45° and 90° phantoms respectively. Any measure with high specificity is a good candidate for classifying the crossing regions. ***Human:*** The *centrum semiovale* was used to illustrate the qualitative analysis of the classification results (Fig. 2). We applied the same classification measures as for the phantom study on the original and denoised data from our datasets. Denoising improves the glyph profiles and the coherence of the non-Gaussian regions, as seen in Fig. 2. We also observe a decrease in the irregularities in the crossing profiles. Going to very high b-values (i.e. >2000s/mm^2) and modeling the data with high SH order (>4) results in polluted glyphs regardless with or without a denoising phase. Comparing the results of the classification from different measures, we observe that increasing the b-value sharpens the HARDI profiles and benefits only for maxima extraction purposes. However, there is no significant gain in classification of non-Gaussian profiles, as observed in the phantom study.

CONCLUSION: From our *ex-vivo* phantom study, we can conclude that CRE, GA and GFA can be applied as a reliable classification between Gaussian and non-Gaussian profiles with in general less than 8% false positive classification results in any configuration. GA and GFA have advantage over CRE since they can be calculated only on the SH coefficients and therefore are significantly faster. An SH order of 4 is sufficient to classify the non-Gaussian profiles. However, if one is interested in the number of maxima, it is then useful to use higher SH order to discriminate low angle crossings, such as 45°. Denoising as a pre-processing step improves the coherence of the classification areas and enhances the HARDI profiles. ADC and q-ball demonstrate strong classification information, even though sometimes lack sufficient angular resolution for small crossing angle discrimination. Increasing the acquisition parameters (b-value >2000s/mm^2 and NG>80) as well as model order, does not significantly improve the classification power. We presented a method that can simplify the data into linear, crossing and isotropic/noise voxels. This means that more sophisticated hybrid methods, which are more time consuming can be applied only in the non-Gaussian areas, whereas linear and isotropic areas can be modeled with a simple diffusion tensor. This classification can reduce the post-processing time and considerably accelerate the visualization of the data. Therefore, this has a potential benefit in clinical settings.

References: [1] Özarslan et al., NeuroImage 36(3):1086-1103, 2006; [2] Tuch, MRM 52(6): 1358-1372, 2004 ; [3] Chen et al., IPMI 246-257, 2005; [4] Descoteaux, PhD thesis 2008; [5] Wedeen et al, MRM 54(6):1377-1386, 2005; [6] Poupon et al, MRM 60: 1276-1283, 2008